

**GREEN SYNTHESIS OF IRON  
NANOPARTICLES FROM *MORINGA OLEIFERA*  
LEAF EXTRACTS: CHARACTERIZATION AND  
APPLICATION FOR DIESEL RANGE ORGANICS  
AND NITRATE REMOVAL**

**UBAH PROMISE CHIMA**

**UNIVERSITI SAINS MALAYSIA**

**2022**

**GREEN SYNTHESIS OF IRON NANOPARTICLES  
FROM *MORINGA OLEIFERA* LEAF EXTRACTS:  
CHARACTERIZATION AND APPLICATION FOR  
DIESEL RANGE ORGANICS AND NITRATE  
REMOVAL**

by

**UBAH PROMISE CHIMA**

**Thesis submitted in fulfilment of the requirements  
for the degree of  
Master of Science**

**August 2022**

## **ACKNOWLEDGEMENT**

I would love to appreciate The Almighty God for the opportunity to carry out this research and for His Grace throughout the research work.

My gratitude also goes to my project supervisor in the person of Professor Rohana Binti Adnan, for her patience, advice and support. I also want to especially thank my parents in the persons of Barr. Uba Jonathan O., (Esq) and Mrs Uba RoseMary for their moral support and financial assistance. My gratitude also goes to Dr Mardiana for her efforts in making sure the analytical procedure was correctly followed and to my fellow research students who have in one way or the other, contributed to the success of this research work.

## TABLE OF CONTENTS

<b>ACKNOWLEDGEMENT</b> .....	<b>ii</b>
<b>TABLE OF CONTENT</b> .....	<b>iii</b>
<b>LIST OF TABLES</b> .....	<b>ix</b>
<b>LIST OF FIGURES</b> .....	<b>xi</b>
<b>LIST OF ABBREVIATIONS</b> .....	<b>xiii</b>
<b>LIST OF APPENDICES</b> .....	<b>xv</b>
<b>ABSTRAK</b> .....	<b>xvii</b>
<b>ABSTRACT</b> .....	<b>xix</b>
<b>CHAPTER 1 INTRODUCTION</b> .....	<b>1</b>
1.1 Background study .....	1
1.2 Problem statement .....	3
1.3 Research objectives .....	5
1.4 Scope of study .....	6
1.5 Hypotheses .....	8
<b>CHAPTER 2 LITERATURE REVIEW</b> .....	<b>9</b>
2.1 Introduction to water pollution.....	9
2.1.1 Surface water pollution .....	10
2.1.2 Groundwater pollution .....	11
2.2 Water treatment methods .....	12
2.2.1 Physical water treatment methods .....	13
2.2.2 Chemical water treatment methods .....	14
2.2.3 Biological water treatment methods .....	15
2.3 Oil and petroleum-related pollution .....	16

2.4	Sources of total petroleum hydrocarbons (TPH) pollution.....	19
2.5	Remediation of TPH from contaminated water .....	19
2.6	Nitrate pollution of water .....	21
2.7	Sources of nitrate pollution .....	22
2.8	Remediation of nitrate from contaminated water.....	24
2.9	Nanoparticles remediation of water pollutants .....	25
2.10	Plant-mediated nanoparticles for contaminated water remediation .....	28
2.11	<i>M. Oleifera</i> plant leaves for green synthesis of nanoparticles .....	30
2.12	Factors affecting the green synthesis of nanoparticles.....	34
2.12.1	pH of plant extracts .....	34
2.12.2	Antioxidant capacity of plants.....	35
2.12.3	Plant extract concentration .....	36
2.12.4	Time and temperature.....	36
<b>CHAPTER 3 MATERIALS AND METHOD .....</b>		<b>37</b>
3.1	Chemicals.....	37
3.2	Procedures .....	38
3.2.1	Sample preparation and drying.....	38
3.2.2	Water and ethanol-based extraction of <i>M. Oleifera</i> leaves .....	39
3.2.3	Determination of total phenolic content of EtOH-MOL and H <sub>2</sub> O-MOL.....	40
3.2.4	Determination of total flavonoids content of EtOH- MOL and H <sub>2</sub> O-MOL.....	40
3.2.5	Fabrication of biosynthesized iron nanoparticles (BINPs) from MOL.....	41
3.3	Instrumental methods and characterization of nanoparticles analysis .....	44
3.3.1	Ultraviolet-Visible spectroscopy .....	44
3.3.2	Fourier transform infrared (FTIR) spectroscopy .....	44

3.3.3	Scanning electron microscopy and energy dispersive X-Ray .....	45
3.3.4	Transmission electron microscopy .....	45
3.3.5	X-Ray diffraction analysis.....	45
3.3.6	Nitrogen adsorption-desorption analysis.....	46
3.4	Preparation of standard solutions, calibration curve and linearity of diesel range organics (DRO) and nitrate-nitrogen (NO <sub>3</sub> -N) standard solutions.....	46
3.4.1	Preparation of DRO standard solutions.....	46
3.4.2	Gas chromatography analysis of the DRO standard solutions .....	48
3.4.3	Linearity .....	50
3.4.4	Preparation of NO <sub>3</sub> -N standard solutions and calibration curve .....	50
3.5	Batch adsorption studies .....	51
3.5.1	Batch study experiments for the removal of DRO using BINPs ..	51
3.5.2	Batch adsorption experiments for the removal of NO <sub>3</sub> -N.....	55
3.6	Adsorption kinetics .....	57
3.7	Equilibrium modelling by adsorption studies .....	57
3.8	Experimental design.....	57
3.9	Reusability studies .....	58
<b>CHAPTER 4 RESULTS AND DISCUSSIONS.....</b>		<b>59</b>
4.1.	Total phenolic content (TPC) of the ethanolic and water extracts of <i>M. Oleifera</i> leaves .....	59
4.2	Total flavonoid contents (TFC) of EtOH-MOL and H <sub>2</sub> O-MOL.....	60
4.3	Fabrication of biosynthesized iron nanoparticles (BINPs) from MOL.....	62
4.4	Characterization results of MOL and BINPs .....	63
4.4.1	Ultraviolet-Visible (UV-Vis) analysis of MOL and BINPs .....	63
4.4.2.	Fourier transform infrared (FTIR) spectroscopy .....	68
4.4.3.	Scanning electron microscopy/energy dispersive X-ray (SEM/EDX) .....	75

4.4.4	Transmission electron microscopy (TEM) analysis.....	80
4.4.5	X-ray diffraction (XRD) analysis.....	82
4.4.6	Nitrogen adsorption- desorption analysis.....	86
4.5	Removal of DRO from contaminated water by BINPs.....	93
4.5.1	Linearity of the calibration curve .....	93
4.5.2	Analysis of method blank.....	93
4.5.3	Accuracy of DRO removal method.....	95
4.6	Effect of reaction parameters on DRO removal from contaminated water using BINPs .....	95
4.6.1	Effect of contact time .....	99
4.6.2	Effect of BINPs dosage .....	101
4.6.3	Effect of initial pH.....	103
4.6.4	Effect of temperature.....	105
4.7	Kinetic modelling.....	107
4.8	Equilibrium modelling of DRO adsorption.....	109
4.9	Removal of NO <sub>3</sub> -N using BINPs from contaminated water .....	113
4.9.1	Linearity .....	113
4.9.2	Effect of contact time .....	114
4.9.3	Effect of BINPs dosage on NO <sub>3</sub> -Nremoval.....	116
4.9.4	Effect of reaction pH .....	118
4.9.5	Effect of temperature.....	120
4.10	Precision of NO <sub>3</sub> -N determination method.....	122
4.11	Accuracy .....	122
4.12	Kinetic modelling.....	123
4.13	Equilibrium modelling .....	126
4.13.1	Adsorption isotherms to describe the adsorption of NO <sub>3</sub> -N onto	

BINPs.....	127
4.14 Experimental design analysis results .....	130
4.14.1 Factorial design analysis for the assessment of factor effects on	130
4.14.2 Optimization design experiment using RSM and modelling .....	136
4.15 Analysis of Variance (ANOVA) of the reduced quadratic model .....	144
4.16 Adsorbent reusability study.....	146
<b>CHAPTER 5 CONCLUSION.....</b>	<b>150</b>
5.1 General conclusion.....	150
5.2 Contribution to knowledge.....	152
5.3 Challenges and future recommendations .....	152
<b>REFERENCES.....</b>	<b>154</b>
<b>APPENDICES</b>	
<b>LIST OF PUBLICATIONS</b>	



## LIST OF TABLES

		Page
Table 2.1	Petroleum product compositions.....	18
Table 2.2	General methods of nanoparticles fabrication.....	26
Table 2.3	Some selected plant materials used for the fabrication of nanoparticles, the shapes, particle sizes, and structure of the nanoparticles.....	29
Table 2.4	Metal precursors, shapes, and particle sizes of <i>M. Oleifera</i> functionalized nanoparticles.....	30
Table 3.1	List of chemicals used in this study and their chemical formulas....	38
Table 3.2	Diesel range organics (DRO) analyte values.....	48
Table 4.1	Total phenolic content of ethanolic and water extract of <i>M. Oleifera</i> plant leaves.....	60
Table 4.2	Total flavonoid content of ethanolic and the water extract of <i>M. Oleifera</i> plant leaves.....	61
Table 4.3	The material yield of BINP <sub>EtOH</sub> and BINP <sub>H<sub>2</sub>O</sub> for different MOL: FeSO <sub>4</sub> .7H <sub>2</sub> O mixing volume ratio of 1:2.....	63
Table 4.4	XRD parameters of iron nanoparticles fabricated from ethanolic <i>M. Oleifera</i> plant leaves extracted with ethanol (BINP <sub>EtOH</sub> ) and water (BINP <sub>H<sub>2</sub>O</sub> ).....	84
Table 4.5	BET surface areas, pore sizes and pore volume distributions BINPs of different iron precursor concentrations.....	87
Table 4.6	Parameters of the calibration curve obtained from the working standards of diesel range organics.....	93
Table 4.7	Recovery analysis of diesel range organics.....	95
Table 4.8	The parameters of adsorption kinetic model for pseudo-first-order kinetics and pseudo-second-order kinetics for the removal of diesel range organics from contaminated water using BINPs.....	109
Table 4.9	The parameters for Langmuir isotherm plot for removal of diesel range organics from contaminated water using <i>M. Oleifera</i> functionalized nanoparticles.....	113

Table 4.10	The parameters for Freundlich isotherm plot for removal of diesel range organics from contaminated water using <i>M. Oleifera</i> functionalized nanoparticles .....113
Table 4.11	Determination of the repeatability of the Ultraviolet-Visible analysis results of NO <sub>3</sub> -N for precision studies.....122
Table 4.12	Recovery assessment of nitrate-nitrogen using Ultraviolet-Visible spectrophotometer for determination of the method accuracy.....123
Table 4.13	Parameters of adsorption kinetic model for pseudo first-order kinetics and pseudo second-order kinetics for the removal of nitrate-nitrogen from contaminated water.....125
Table 4.14	The parameters for Langmuir isotherm plot of <i>M. Oleifera</i> functionalized nanoparticles for removal of nitrate-nitrogen from contaminated water.....129
Table 4.15	The parameters for Freundlich isotherm plot of <i>M. Oleifera</i> functionalized nanoparticles for removal of nitrate-nitrogen from contaminated water.....129
Table 4.16	The experimental matrix for response surface assessment of <i>M. Oleifera</i> functionalized nanoparticles (BINPs) for the optimization of statistically significant factors affecting the adsorption of DRO by BINPs.....136
Table 4.17	The experimental matrix for response surface assessment of <i>M. Oleifera</i> functionalized nanoparticles (BINPs) for the optimization of statistically significant factors affecting the adsorption of NO <sub>3</sub> -N by BINPs.....141
Table 4.18	Analysis of Variance for examination of the reduced quadratic model adequacy on adsorption efficiency of <i>M. Oleifera</i> functionalized iron nanoparticles to remove DRO from contaminated water.....145
Table 4.19	Analysis of Variance for examination of the reduced quadratic model adequacy on adsorption efficiency of <i>M. Oleifera</i> functionalized iron nanoparticles to remove NO <sub>3</sub> -N from contaminated water.....145

## LIST OF FIGURES

	<b>Page</b>
Figure 1.1	Daily oil consumption from 1980 to 2006 2006 (Source: the US energy information administration)..... 4
Figure 2.1	Percentage distribution of the earth's ..... 9
Figure 2.2	Classification of water treatment technologies for the removal of pollutants with examples ..... 12
Figure 2.3	Structure of a nitrate molecule ..... 20
Figure 2.4	Diagram showing sources of nitrate pollution of water..... 22
Figure 2.5	A flowchart for a general method for plant-mediated synthesis of nanoparticles..... 27
Figure 2.6	<i>M. Oleifera</i> plant and its fruits..... 30
Figure 3.1	Schematic illustration of BINPs synthesis, characterization and analysis used in this study..... 44
Figure 4.1	UV spectra of (a) H <sub>2</sub> O-MOL and 0.1 M BINP <sub>SH<sub>2</sub>O</sub> (b) EtOH-MOL and 0.1 M BINP <sub>SEtOH</sub> (c) FeSO <sub>4</sub> , 0.1 M BINP <sub>SEtOH</sub> and BINP <sub>SH<sub>2</sub>O</sub> ..... 66
Figure 4.2	FTIR spectra of <i>M. Oleifera</i> extract showing (a) EtOH-MOL (b) H <sub>2</sub> O-MOL..... 71
Figure 4.3	FTIR spectra of (a) FeSO <sub>4</sub> (b) EtOH-MOL (c) 0.1 M BINP <sub>SEtOH</sub> (d) H <sub>2</sub> O-MOL (d) 0.1 M BINP <sub>SH<sub>2</sub>O</sub> ..... 72
Figure 4.4	FTIR spectra of (a) 0.05 M BINP <sub>SEtOH</sub> , (b) 0.1 M BINP <sub>SEtOH</sub> , (c) 0.25 M BINP <sub>SEtOH</sub> , (d) 0.5 M BINP <sub>SEtOH</sub> ..... 73
Figure 4.5	FTIR spectra of (a) 0.05 M BINP <sub>SH<sub>2</sub>O</sub> , (b) 0.1 M BINP <sub>SH<sub>2</sub>O</sub> , (c) 0.25 M BINP <sub>SH<sub>2</sub>O</sub> , (d) 0.5 M BINP <sub>SH<sub>2</sub>O</sub> ..... 74
Figure 4.6	SEM micrographs with resolutions of 200×, 1500× and EDX spectra/elemental composition of (i) 0.05 M BINP <sub>SEtOH</sub> [(a), (b), (c)], (ii) 0.1 M BINP <sub>SEtOH</sub> [(d), (e), (f)], (iii) 0.25 M BINP <sub>SEtOH</sub> [(g), (h), (i)], (iv) 0.5 M BINP <sub>SEtOH</sub> [(j), (k), (l)]..... 76
Figure 4.7	SEM micrographs with resolutions of 200×, 1500× and EDX spectra/elemental composition of (i) 0.05 M BINP <sub>SH<sub>2</sub>O</sub> [(a), (b), (c)],

	(ii) 0.1 M BINP <sub>SH<sub>2</sub>O</sub> [(d), (e), (f)], (iii) 0.25 M BINP <sub>SH<sub>2</sub>O</sub> [(g), (h), (i)], (iv) 0.5 M BINP <sub>SH<sub>2</sub>O</sub> [(j), (k), (l)].....	78
Figure 4.8	TEM micrographs (resolution: 50k) of (a) 0.05 M iron nanoparticles synthesized from ethanolic extract of <i>M. Oleifera</i> (BINP <sub>SEtOH0.05</sub> ) (b) 0.5 M iron nanoparticles synthesized from ethanolic extract of <i>M. Oleifera</i> (BINP <sub>SEtOH0.5</sub> ) (c) 0.05 M iron nanoparticles synthesized from water extract of <i>M. Oleifera</i> (BINP <sub>SH<sub>2</sub>O0.05</sub> ) (d) 0.5 M iron nanoparticles synthesized from ethanolic extract of <i>M. Oleifera</i> (BINP <sub>SH<sub>2</sub>O0.5</sub> ).....	82
Figure 4.9	XRD diffractograms of (a) 0.05 M BINP <sub>SEtOH</sub> (b) 0.1 M BINP <sub>SEtOH</sub> (c) 0.25 M BINP <sub>SEtOH</sub> (d) 0.5 M BINP <sub>SEtOH</sub> (e) 0.05 M BINP <sub>SH<sub>2</sub>O</sub> (f) 0.1 M BINP <sub>SH<sub>2</sub>O</sub> (g) 0.25 M BINP <sub>SH<sub>2</sub>O</sub> (h) 0.5 M BINP <sub>SH<sub>2</sub>O</sub> .....	85
Figure 4.10	BET nitrogen adsorption-desorption isotherm curves of (a) FeSO <sub>4</sub> .7H <sub>2</sub> O (b) BINP <sub>SH<sub>2</sub>O0.05</sub> (c) BINP <sub>SH<sub>2</sub>O0.1</sub> (d) BINP <sub>SH<sub>2</sub>O0.25</sub> (e) BINP <sub>SH<sub>2</sub>O0.5</sub> (f) BINP <sub>SEtOH0.05</sub> (g) BINP <sub>SEtOH0.1</sub> (h) BINP <sub>SEtOH0.25</sub> (i) BINP <sub>SEtOH0.5</sub> .....	88
Figure 4.11	Chromatograms of 1 microlitre injections of (a) solvent blank solution (b) method blank solution.....	94
Figure 4.12	Chromatogram of a 1 µL injection of (a) the DRO standard solution at 100 µg mL <sup>-1</sup> obtained with the conventional split inlet (b) DRO after treatment with BINPs (C <sub>i</sub> = 100 µg mL <sup>-1</sup> , C <sub>f</sub> = 14.3 µg mL <sup>-1</sup> , T = 35°C, pH = 8) (c) the DRO standard solution at 50 µg mL <sup>-1</sup> obtained with the conventional split inlet, (d) DRO after treatment with BINPs (C <sub>i</sub> = 50 µg mL <sup>-1</sup> , C <sub>f</sub> = 5.8 µg mL <sup>-1</sup> , T = 35°C, pH = 8), (e) the DRO standard solution at 100 µg mL <sup>-1</sup> obtained with the conventional split inlet.	96
Figure 4.13	Effect of contact time on DRO removal using (a) BINP <sub>SEtOH</sub> (b) BINP <sub>H<sub>2</sub>O</sub> (C <sub>0</sub> = 20 µg mL <sup>-1</sup> , Dose = 1 g, T = 30°C, pH = 6.5).....	100
Figure 4.14	Effect of dosage on DRO removal using (a) BINP <sub>SEtOH</sub> (b) BINP <sub>H<sub>2</sub>O</sub> (C <sub>0</sub> = 20 µg mL <sup>-1</sup> , Time = 1 hr, T = 30°C, pH = 6.5).....	102
Figure 4.15	Effect of pH on DRO removal using (a) BINP <sub>SEtOH</sub> (b) BINP <sub>H<sub>2</sub>O</sub> (C <sub>0</sub> = 20 µg mL <sup>-1</sup> , Time = 1 hr, Dose = 1 g, T = 30°C).....	104
Figure 4.16	Effect of temperature on DRO removal using (a) BINP <sub>SEtOH</sub> (b) BINP <sub>H<sub>2</sub>O</sub> (C <sub>0</sub> = 20 µg mL <sup>-1</sup> , Time = 1 hr, Dose = 1 g, pH = 6.5).....	106

Figure 4.17	Kinetic models of the biosynthesized nanoparticles for; (a) Pseudo first order kinetic model of (b) Pseudo second order kinetic model of BINPs for DRO adsorption.....	108
Figure 4.18	(a) Langmuir isotherm plot of $\text{BINP}_{\text{SEtOH}}$ on DRO removal (b) Langmuir isotherm of $\text{BINP}_{\text{SH}_2\text{O}}$ on DRO removal (c) Freundlich isotherm plot of $\text{BINP}_{\text{SEtOH}}$ on DRO removal (b) Freundlich isotherm plot on $\text{NO}_3\text{-N}$ removal.....	111
Figure 4.19	Effect of contact time on the adsorption of $\text{NO}_3\text{-N}$ using (a) $\text{BINP}_{\text{SEtOH}}$ (b) $\text{BINP}_{\text{H}_2\text{O}}$ ( $C_0 = 30 \text{ mg L}^{-1}$ , Dose = 1 g, pH = 6.5, T = $30^\circ\text{C}$ ).....	115
Figure 4.20	Effect of dosage time on the adsorption of $\text{NO}_3\text{-N}$ using (a) $\text{BINP}_{\text{SEtOH}}$ (b) $\text{BINP}_{\text{H}_2\text{O}}$ ( $C_0 = 30 \text{ mg L}^{-1}$ , time = 1 hr, pH = 6.5, T = $30^\circ\text{C}$ ).....	117
Figure 4.21	Effect of pH on the adsorption of $\text{NO}_3\text{-N}$ using (a) $\text{BINP}_{\text{SEtOH}}$ (b) $\text{BINP}_{\text{H}_2\text{O}}$ ( $C_0 = 30 \text{ mg L}^{-1}$ , Dose = 1 g, time = 1 hr, T = $30^\circ\text{C}$ ).....	119
Figure 4.22	Effect of temperature on the adsorption of $\text{NO}_3\text{-N}$ using (a) $\text{BINP}_{\text{H}_2\text{O}}$ (b) $\text{BINP}_{\text{SEtOH}}$ ( $C_0 = 30 \text{ mg L}^{-1}$ , Dose = 1 g, pH = 6.5, time = 1 hr).....	120
Figure 4.23	Kinetic models of the of the adsorption of $\text{NO}_3\text{-N}$ using BINPs ( $C_0 = 20 \mu\text{g mL}^{-1}$ , pH = 6.5, T = $30^\circ\text{C}$ , W = 1 g $\text{L}^{-1}$ , V = 100 mL) for (a) Pseudo first order kinetic model (b) Pseudo second order kinetic...	124
Figure 4.24	Langmuir adsorption isotherm plots for (a) $\text{NO}_3\text{-N}$ removal using biosynthesized nanoparticles from ethanolic extract of <i>M. Oleifera</i> ( $\text{BINP}_{\text{SEtOH}}$ ) (b) $\text{NO}_3\text{-N}$ removal using biosynthesized nanoparticles from water extract of <i>M. Oleifera</i> ( $\text{BINP}_{\text{SH}_2\text{O}}$ ).....	127
Figure 4.25	Freundlich adsorption isotherm plots for (a) $\text{NO}_3\text{-N}$ removal using biosynthesized nanoparticles from ethanolic extract of <i>M. Oleifera</i> ( $\text{BINP}_{\text{SEtOH}}$ ) (b) $\text{NO}_3\text{-N}$ removal using biosynthesized nanoparticles from water extract of <i>M. Oleifera</i> ( $\text{BINP}_{\text{SH}_2\text{O}}$ ).....	128
Figure 4.26	Half-normal plots (a,b), normal plots (c,d) and Pareto charts (e,f) of models ( $\alpha = 0.05$ ) for adsorption of DRO and $\text{NO}_3\text{-N}$ by BINPs, respectively.....	132
Figure 4.27	3D surface plots of a (a) 2D contour plot (b) actual versus predicted adsorption efficiency plot (c) and ramps (d-g) of BINPs for the adsorption of DRO.....	138

Figure 4.28	3D surface plots of a (a) 2D contour plot (b) actual versus predicted adsorption efficiency plot (c) of BINPs for the adsorption of NO <sub>3</sub> -N.....	142
Figure 4.29	Regeneration study graph for the adsorption-desorption of (a) DRO onto BINP <sub>SH2O0.5</sub> (b) DRO onto BINP <sub>SEtOH0.5</sub> (c) NO <sub>3</sub> -N onto BINP <sub>SH2O0</sub> (d) NO <sub>3</sub> -N onto BINP <sub>SEtOH0.5</sub> (pH = 6.5, T = 30°C, C <sub>0</sub> = 1 g).....	147

## LIST OF ABBREVIATIONS

BINPs	Biosynthesized Iron Nanoparticles
$C_e$	Equilibrium Concentration of DRO (mg mL <sup>-1</sup> )
$C_i$	Initial DRO concentration (μg mL <sup>-1</sup> )
C.V	Calibration Verification
DAF	Dissolved Air Flotation
DRO	Diesel Range Organics
GC-FID	Gas Chromatography fitted with Flame Ionization Detector
INPs	Iron Nanoparticles
IS	Internal Standard
$k_1$	Rate constant of pseudo-first-order kinetic model (min <sup>-1</sup> )
$k_2$	Rate constant of pseudo-second-order model (g mg.min <sup>-1</sup> )
$K_f$	Freundlich constant indicating adsorption capacity (mg g <sup>-1</sup> )/(L mg <sup>-1</sup> ) <sup>1/n</sup>
$K_L$	Langmuir constant (L mol <sup>-1</sup> )
MCLG	Maximum contaminant level goal
MCL	Maximum contaminant level
MOL	<i>Moringa Oleifera</i> leaf extract
$n$	Freundlich isotherm model constant (L mg <sup>-1</sup> )
NPs	Nanoparticles
PMNPs	Plant-Mediated nanoparticles
$q_{Cal}$	Calculated equilibrium adsorption capacity (mg g <sup>-1</sup> )

$q_e$	Equilibrium adsorption ( $\text{mg g}^{-1}$ )
$q_m$	Maximum monolayer adsorption ( $\text{mg g}^{-1}$ )
$R^2$	Regression coefficient
$R1$	Response 1
$R2$	Response 2
RSM	Response Surface Methodology
$T$	Temperature
TPH	Total Petroleum Hydrocarbons
US EPA	The United States Environmental Protection Agency
$V$	Working volume (L)
$W$	Adsorbent weight (g)
ZNPs	Zerovalent nanoparticles
ZINPs	Zerovalent iron nanoparticles



## LIST OF APPENDICES

- APPENDIX A Calibration curve of quercetin for quantitation of TFC of BINPs.
- APPENDIX B: Calibration curve of working standards of DRO
- APPENDIX C Calibration curve of NO<sub>3</sub>-N
- APPENDIX D: UV spectrum of NO<sub>3</sub>-N showing  $\lambda_{max}$  at ~220 nm
- APPENDIX E: XRD spectra of (a) 0.05 M BINP<sub>SEtOH</sub> (b) 0.1 M BINP<sub>SEtOH</sub> (C) 0.25 M BINP<sub>SEtOH</sub> (D) 0.5 M BINP<sub>SEtOH</sub> (e) 0.05 M BINP<sub>SH<sub>2</sub>O</sub> (F) 0.1 M BINP<sub>SH<sub>2</sub>O</sub> (G) 0.25 M BINP<sub>SH<sub>2</sub>O</sub> (H) 0.5 M BINP<sub>SH<sub>2</sub>O</sub>.
- APPENDIX F Chromatograms of 1 microlitre injections of DRO calibration standards at (A) 1  $\mu\text{g/mL}$  (B) 2  $\mu\text{g mL}^{-1}$  (C) 5  $\mu\text{g mL}^{-1}$  (D) 10  $\mu\text{g mL}^{-1}$  (E) 20  $\mu\text{g mL}^{-1}$  (F) 50  $\mu\text{g mL}^{-1}$  and (G) 100  $\mu\text{g mL}^{-1}$ .

**SINTESIS HIJAU NANOPARTIKEL FERUM DARI EKSTRAK DAUN  
*MORINGA OLEIFERA*: PENCIRIAN DAN APLIKASI UNTUK  
PENYINGKIRAN SEBATIAN ORGANIK DIESEL DAN NITRAT**

**ABSTRAK**

Ekstrak daun tumbuhan *Moringa Oleifera* (*M. Oleifera*) berasaskan etanol (EtOH-MOL) dan ekstrak berasaskan air (H<sub>2</sub>O-MOL) digunakan dalam kajian ini untuk biosintesis nanopartikel ferum (BINPs). *M. Oleifera* adalah tumbuhan tropika tidak beracun yang terkenal dengan khasiat perubatannya dan kandungan antioksidan yang baik. Ferum sulfat heptahidrat digunakan sebagai garam prekursor untuk pembentukan BINPs. Ferum merupakan pilihan yang menarik kerana ia murah, tidak beracun, dan mudah didapati. Nanopartikel ferum yang disintesis dari EtOH-MOL (BINP<sub>SEtOH</sub>), dan H<sub>2</sub>O-MOL (BINP<sub>SH<sub>2</sub>O</sub>) dicirikan dan keberkesanannya dalam rawatan air tercemar dikaji terhadap penyingkiran sebatian organik diesel (DRO) dan nitrat-nitrogen (NO<sub>3</sub><sup>-</sup>N) dari sampel air buangan tersimulasi dibawah parameter tindak balas yang berbeza seperti suhu (25 – 45°C), pH (4 – 8), dos (0.1 – 2 g), dan masa sentuhan (2 – 8 jam) dalam eksperimen kelompok. Sampel air terawat dianalisa menggunakan kromatografi gas yang dilengkapi dengan pengesan nyalaan pengionan (GC-FID) untuk analisis DRO dan spektrofotometer UV cahaya tampak untuk analisis NO<sub>3</sub><sup>-</sup>N. Jumlah kandungan fenolik (TPC) bagi EtOH-MOL dan H<sub>2</sub>O-MOL yang diperoleh dalam kajian ini didapati masing-masing adalah 47.98 ± 0.03 dan 27.82 ± 0.12 mg setara asid galik (GAE) per g ekstrak. Sementara itu, kandungan flavonoid (TFC) masing-masing adalah 11.30 ± 0.06 dan 3.59 ± 0.15 mg setara dengan quercetin

(QE) per g sampel kering. Pencirian keatas BINPs menunjukkan pembentukan nanosfera dan nanokub dengan ukuran zarah purata  $50.9 \pm 9.7$  dan  $42.3 \pm 7.2$  nm bagi  $\text{BINP}_{\text{SEtOH}}$  dan  $\text{BINP}_{\text{SH}_2\text{O}}$  masing-masing. Analisis EDX mendedahkan bahawa komposisi Fe dan O dalam BINPs adalah  $16.78 \pm 4.26$  dan  $38.09 \pm 3.64$  peratus berat yang menyokong kehadiran antioksidan dari ekstrak tumbuhan.  $\text{BINP}_{\text{SEtOH}}$  merupakan penjerap yang lebih baik bagi penyingkiran kedua-dua DRO dan  $\text{NO}_3\text{-N}$ . Sifat penjerapan BINPs dikaji menggunakan model isoterma penjerapan Langmuir dan Freundlich sementara kinetik penjerapan dimodelkan dengan menggunakan model kinetik pseudo tertib pertama dan model kinetic pseudo tertib kedua. Data keseimbangan eksperimen bagi  $\text{BINP}_{\text{SEtOH}}$  dan  $\text{BINP}_{\text{SH}_2\text{O}}$  terhadap penyingkiran DRO sangat bersesuaian dengan isoterma penjerapan Langmuir (masing-masing  $R^2 = 0.999$  dan  $0.993$ ) dengan liputan monolapisan maksimum masing-masing  $7.19$  dan  $8.33$   $\text{mg g}^{-1}$ . Perkara yang sama turut dilihat bagi penyingkiran  $\text{NO}_3\text{-N}$ , bagaimanapun liputan monolapisan maksimum masing-masing adalah lebih rendah iaitu  $3.91$  dan  $1.45$   $\text{mg g}^{-1}$ . Kinetik penjerapan bagi BINPs mematuhi model kinetik pseudo tertib kedua. Analisis reka bentuk faktorial dua peringkat digunakan untuk menentukan pemboleh ubah yang mempengaruhi kecekapan penjerapan BINPs yang signifikan secara statistik sementara reka bentuk komposit sentral dari metodologi permukaan tindak balas digunakan untuk permodelan dan pengoptimuman pemboleh ubah yang signifikan secara statistik.

**GREEN SYNTHESIS OF IRON NANOPARTICLES FROM *MORINGA*  
*OLEIFERA* LEAF EXTRACTS: CHARACTERIZATION AND  
APPLICATION FOR DIESEL RANGE ORGANICS AND NITRATE  
REMOVAL**

**ABSTRACT**

Ethanollic extract (EtOH-MOL) and water extract (H<sub>2</sub>O-MOL) of *Moringa Oleifera* (*M. Oleifera*) plant leaves were used in this study for the biosynthesized iron nanoparticles (BINPs). *M. Oleifera* is a non-toxic tropical plant known for its medicinal properties and good antioxidant content. Iron sulphate heptahydrate was used as the metal precursor for the formulation of BINPs. Iron is of interest because it is cheap, non-toxic, and readily available. Iron nanoparticles synthesized from EtOH-MOL (BINP<sub>SEtOH</sub>) and H<sub>2</sub>O-MOL (BINP<sub>SH<sub>2</sub>O</sub>), were characterized and their efficiencies in the remediation of contaminated water were investigated for the removal of diesel range organics (DRO) and nitrate-nitrogen (NO<sub>3</sub>-N) from simulated wastewater samples under different reaction parameters such as temperature (25 – 55°C), pH (4 – 10), dosage (0.1 – 2 g), and contact time (2 – 8 hr) in batch experiments. The treated water samples were characterized using gas chromatography fitted with flame ionization detector (GC-FID) for the analysis of DRO and UV-visible spectrophotometer for the analysis of NO<sub>3</sub><sup>-</sup>N. The total phenolic content (TPC) of EtOH-MOL and H<sub>2</sub>O-MOL obtained in this study were found to be 47.98 ± 0.03 and 27.82 ± 0.12 mg of gallic acid equivalent (GAE)/g of extract, respectively. Meanwhile, the flavonoids contents (TFC) were 11.30 ± 0.06 and 3.59 ± 0.15 mg of quercetin equivalent (QE)/g of dried sample, respectively. The characterization revealed the

formation of nanospheres and nanocubes with an average particle size of  $50.9 \pm 9.7$  and  $42.3 \pm 7.2$  nm, for BINP<sub>SEtOH</sub> and BINP<sub>SH<sub>2</sub>O</sub>, respectively. EDX analysis revealed that the composition of Fe and O in BINPs was  $16.78 \pm 4.26$  and  $38.09 \pm 3.64$  by weight per cent which confirms the presence of antioxidants from the plant extract. BINP<sub>SEtOH</sub> was found to be a better adsorbent for both DRO removal and NO<sub>3</sub>-N removal. The adsorption properties of the BINPs were studied using Langmuir and Freundlich isotherm models while the adsorption kinetics were modelled by employing the pseudo-first and second-order kinetics model. Experimental equilibrium data for BINP<sub>SEtOH</sub> dan BINP<sub>SH<sub>2</sub>O</sub> on the removal of DRO fit the Langmuir adsorption isotherm ( $R^2 = 0.999$  dan  $0.993$ , respectively) with the maximum monolayer coverages of  $7.19$  dan  $8.33$  mg g<sup>-1</sup>, respectively. Similar behaviour was observed for the removal of NO<sub>3</sub>-N but the maximum monolayer coverage was much lower,  $3.91$  and  $1.45$  mg g<sup>-1</sup>, respectively. The adsorption kinetics of BINPs followed the pseudo-second-order kinetics. The two-level factorial design analysis was used to determine the statistically significant variables affecting the adsorption efficiency of BINPs while the central composite design of the response surface methodology was employed for the modelling and optimization of the statistically significant parameters.

## CHAPTER ONE

### INTRODUCTION

#### 1.1 Background study

Water is an essential commodity for all living things. Living organisms depend on water to survive. Hence, pollution of surface water, groundwater and other water sources has inevitably been of major concern. Water pollution occurs when contaminants are introduced into the surface water or groundwater, thereby making the water unfit for consumption or causing degradation of the aquatic ecosystem (Gautam *et al.*, 2019a; Muralikrishna & Manickam, 2017). There are several water pollutants such as pesticides, heavy metals, petroleum hydrocarbons, nitrate etc., that has raised the importance of water remediation (Bhattacharya *et al.*, 2018). Two main sources of water pollution are point source and non-point source. Point source pollution refers to water pollution involving pollutants that find their way to waterbodies via one identifiable source such as a water pipe while non-point source pollution refers to a situation where water bodies are contaminated by multiple sources that cannot be easily identified.

Nutrient pollutants and petroleum pollutants consist of the major pollutants in the ecosystem. Petroleum and its derivatives are widely used in areas of electricity, transportation, agriculture and road construction. This wide application of petroleum products has inevitably caused major environmental pollution and poses a serious challenge to both the ecosystem and human health. Exposure to petroleum hydrocarbon (PHCs) pollutants have been reported to cause pulmonary abnormalities, psychological problems, cancer, changes in cognitive functions, renal and hepatic

problems, etc. Nitrate contamination of water is another major source of water pollution. Nitrate is an important nutrient in water and soil but poses a serious challenge when in high concentrations (Pennino *et al.*, 2017; Ward *et al.*, 2018). Nitrate forms as a result of denitrification of nitrogen and is hence referred to as “nitrate-nitrogen” (NO<sub>3</sub>-N). High levels of NO<sub>3</sub>-N in water can be a result of runoff or leakage from fertilized soil, wastewater, landfills, animal feedlots, septic systems, or urban drainage. NO<sub>3</sub>-N has been reported to be carcinogenic and causes blue baby syndrome; a disease that causes the skin of infants to turn blue (Majumdar, 2003).

The physical methods of water remediation of petroleum and nitrate contaminated waterbodies have proven insufficient due to the high cost of the methods, high energy requirements and secondary pollution. In the modern context of water remediation, the use of nanoparticles has proven efficient and cost-effective. However, the use of chemical precursors in the production of these nanoparticles is a major drawback.

Researchers have found a breakthrough in the use of nanoparticles synthesized from plant or biological materials. The plant-mediated synthesis of nanoparticles otherwise referred to as the green or biosynthesized synthesis of nanoparticles ensures an environmentally friendly and cost-effective way of water remediation. The antioxidants such as polyphenols and flavonoids found in the plant starting materials provide the necessary reduction environment for the reduction of the metal precursors to zerovalent metal nanoparticles in the production of biosynthesized nanoparticles (BNPs). These antioxidants are also responsible for the stabilization of the nanoparticles. The antioxidants stabilize the nanoparticles by reducing the metal ion precursors to zerovalent metals which are in a lower energy state than the metal ions. The stabilization of these metal precursors prevents the agglomeration of the

nanoparticles. Hence, the antioxidants are also referred to as stabilizing or capping agents. The biosynthesized nanoparticles possess large surface areas and porosity and are consequently applied as nanosorbent for the adsorption of water contaminants. Biosynthesized nanoparticles are also capable of degradation of organic water contaminants. The reaction mechanism of nanoparticles that leads to degradation of organic contaminants could be by Fenton oxidation as suggested by researchers (Murgueitio *et al.*, 2018) which is an oxidation process activated by  $\text{Fe}^{2+}$  in the presence of hydrogen peroxide where radical species are generated in solution and oxidizes a wide range of organic substrates with high activity.

In this study, plant-mediated iron nanoparticles (BINPs) were synthesized using *M. Oleifera* plant leaves and ferrous sulphate ( $\text{FeSO}_4 \cdot 7\text{H}_2\text{O}$ ) as the plant starting material and metal precursor, respectively. The synthesized nanoparticles were characterized and applied as a nanosorbent for the removal of DRO and  $\text{NO}_3\text{-N}$  from contaminated water. Adsorption isotherms and adsorption kinetics were used to determine the maximum adsorption capacity, conclude monolayer or multilayer adsorption and to determine the rate of adsorption of the BINPs, respectively. The statistically significant factors that affect the reaction rate were determined by statistical analysis using the regular two-level factorial design analysis and optimization of the explanatory variables was done using the central composite design of the response surface methodology.

## **1.2 Problem statement**

Water is an essential commodity and is required by every living organism for life sustenance. Hence, the pollution of water bodies is a major concern to both humans and beyond as it poses a considerable threat to terrestrial and aquatic life. Nitrate-



nitrogen ( $\text{NO}_3\text{-N}$ ), and total petroleum hydrocarbons (TPH) are very important in our everyday lives. Petroleum is largely used as a source of energy. It is widely used in areas of electricity, transportation, and road construction. It is also used as feedstock in making chemicals, plastics, and synthetic materials that are in nearly everything we use. However, petroleum-derived contaminants constitute one of the most prevalent sources of environmental degradation in the industrialized world. In large concentrations, the hydrocarbon molecules that make up crude oil and petroleum products are highly toxic to many organisms, including humans (Wang *et al.*, 2017).

$\text{NO}_3\text{-N}$  plays a very important role in the human body. They are antimicrobials in the digestive system and also help in neurotransmission, immunity, and blood flow.  $\text{NO}_3\text{-N}$  is an essential nutrient for the growth of plants. However, high levels of nitrates are a cause of many health problems such as cancer. Excess nitrates in water cause eutrophication leading to dramatic growth increase in aquatic plants and destabilization of the aquatic ecosystem.

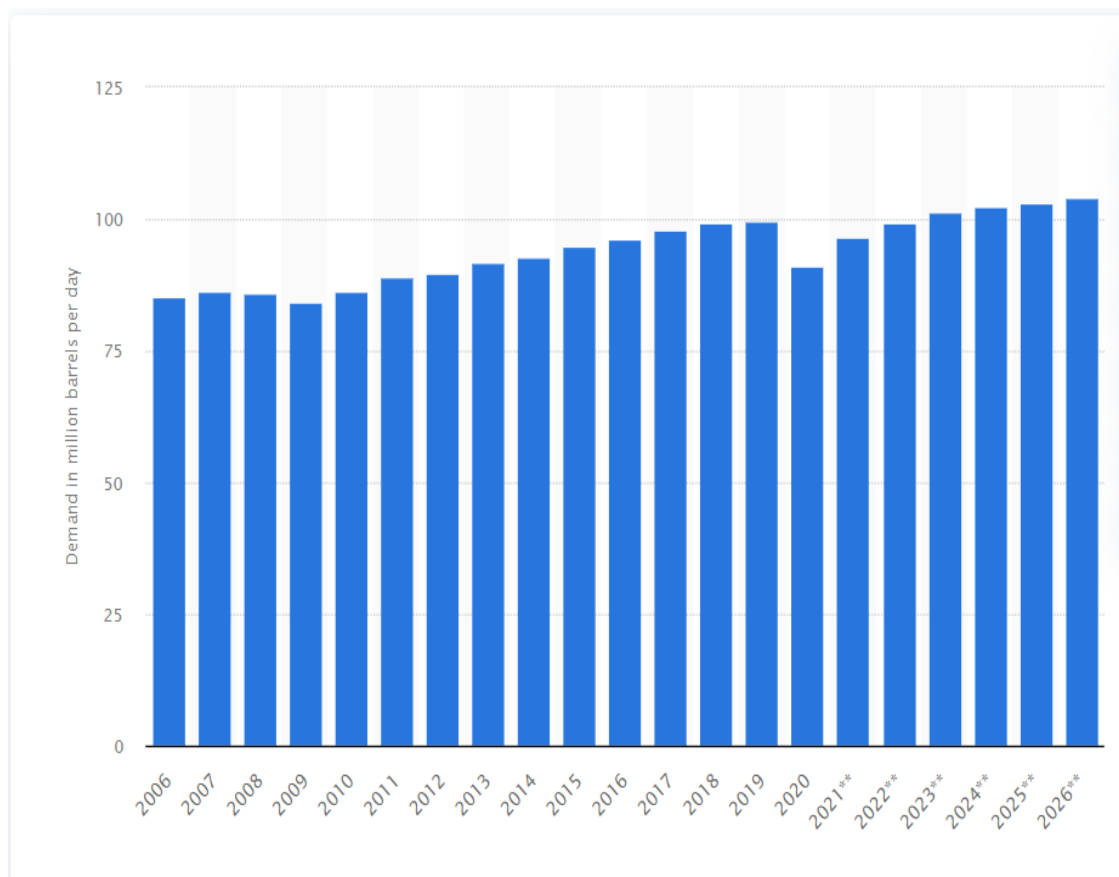


**Fig. 1.1** Daily oil consumption from 2016 to 2020 with a forecast until 2026 (Source: Statista.com).

Conventional methods of water body remediation for  $\text{NO}_3\text{-N}$  removal are costly, complicated, and not completely environmentally friendly. However, the use of biosynthesized nanomaterials in water remediation may promise a cost-effective and environmentally friendly way of treating contaminated water.

### 1.3 Research objectives

Generally, the objective of this work is to provide an environmentally-friendly nanosorbent for the remediation of DRO and  $\text{NO}_3\text{-N}$  from contaminated water. This present study aims to:

- (1) Synthesize and characterize plant-mediated iron nanoparticles (BINPs) as nanosorbent using *M. Oleifera* leaf extracts as the reducing and capping agent for the

iron precursor, for the novel adsorption of TPH (DRO) and NO<sub>3</sub>-N contaminants in water under different conditions.

(2) Investigate the adsorption of DRO and NO<sub>3</sub>-N onto the surface of BINPs under different conditions such as temperature, pH, adsorbent dosage, and contact time for the different iron precursor concentrations to select the best nanosorbent for equilibrium and kinetic modelling,

(3) Determine the BINPs' maximum adsorption capacity and rate determining step using isotherm and kinetic models.

(4) Optimize the statistically significant main and interaction explanatory factors affecting the adsorption efficiency of BINPs for DRO and NO<sub>3</sub>-N remediation of contaminated water using the central composite design of response surface methodology, and develop a fitting model for the prediction of the responses.

#### **1.4 Scope of study**

This research work focuses on the synthesis of iron nanoparticles from *M. Oleifera* leaves using FeSO<sub>4</sub>.7H<sub>2</sub>O precursor, characterization of the synthesized nanoparticles, and remediation of DRO and NO<sub>3</sub>-N from contaminated water. The work done in this study can be categorized into four parts;

- (i) Extraction of *M. Oleifera* leaf extracts (MOL)
- (ii) Fabrication of the biosynthesized nanoparticles (BINPs)
- (iii) Removal of Diesel Range Organics (DRO) from contaminated water, and
- (iv) Removal of NO<sub>3</sub>-N from contaminated water.

In the first part, the efficiency of the MOL extraction routes using water and ethanolic was evaluated based on the leaves' drying techniques and the resulting antioxidant contents (polyphenols and flavonoids). This was aimed to increase the reduction and stabilization of the zerovalent iron and reduce the agglomeration of the BINPs in powdered form.

The second part involved the synthesis of BINPs with a varied mixing volume ratio of MOL:FeSO<sub>4</sub>.7H<sub>2</sub>O and temperature as optimization parameters to determine the best yield of BINPs. The synthesized iron nanoparticles will be characterized using techniques such as UV-visible spectroscopy, X-ray diffraction, Fourier transform infra-red spectroscopy, scanning electron microscopy/ energy dispersive X-ray analysis, and N<sub>2</sub> adsorption-desorption isotherms to determine the absorption peaks, morphology, size, shape and porosity of the synthesized nanoparticles. Upon completion, the effectiveness of the synthesized nanoparticles to degrade and adsorb NO<sub>3</sub>-N from contaminated water samples will be monitored using GC-FID and UV-Visible spectrophotometer as the analytical tools for determination of the DRO and NO<sub>3</sub>-N concentration in the contaminated water before and after treatment with the synthesized iron nanoparticles respectively, under different conditions for optimization. Adsorption isotherms and adsorption kinetics will be used to investigate the maximum adsorption capacity and the rate of adsorption of the BINPs. Statistical analysis will be used to determine the statistically significant independent variables affecting the adsorption efficiency of the BINPs. Response surface methodology will be employed for the optimization of the statistically significant independent variables using the central composite design analysis.

## 1.5 Hypotheses

Iron nanoparticles synthesized from *M. Oleifera* plant leaves are expected to show a statistically significant tendency of adsorption of DRO from contaminated water with increasing retention time, temperature, pH, and dosage of the adsorbent.

Iron nanoparticles synthesized from *M. Oleifera* plant leaves are expected to show a statistically significant tendency towards the adsorption of NO<sub>3</sub>-N from contaminated water with increasing retention time, temperature, pH, and dosage of the adsorbent. The iron nanoparticles are stable and reusable adsorbents for the adsorption of DRO and NO<sub>3</sub>-N.

## CHAPTER TWO

### LITERATURE REVIEW

#### 2.1 Introduction to water pollution

Water is an essential commodity for all living things and constitutes 70.8% of the earth's surface yet. However, just a small percentage of the earth's water is available for municipal and industrial use (McLellan *et al.*, 2018; Statista, 2019). From Fig. 2.1, it can be seen that oceans comprise over 96% of the earth's water which is very saline and cannot be used for human consumption or growing plants. Just 2.5% of the earth's water is freshwater, and only 1.3% of all freshwater is surface water which serves most of life's needs. Most of this surface water (73.1%) is locked up in ice and another 20.1%, in lakes. In general, only about 0.3% of the earth's water is available for human consumption. Yet, much of the 0.3% of usable water is unattainable. The use of this small percentage of water available for human consumption is further limited by pollution. The recently increased levels of water consumption and correspondingly high levels of water pollution have generated a paramount need for maintaining good water quality. It is reported that 844 million people in the world are still lacking basic drinking water services (WHO & UNICEF, 2017).

Water pollution occurs in many ways which can be grouped into two; point sources and non-point sources. The point sources of pollution entail pollution from one identifiable source like a wastewater pipe while non-point pollution describes pollution from multiple sources that are not easily identified. Most water pollution is due to non-point sources which makes it difficult to locate the source of pollution and the remediation, more costly. Oil-related water pollution and nutrient pollution are two

of the water pollution types that have raised major concerns. It is reported that every year, there are about 3,000 incidents involving oil and fuel pollution in England and Wales (Philippines Environment Monitor, 2003). Oil pollution can be a result of deliberate disposal of oil waste to drainage systems, spillage or loss from storage facilities. Oil pollution is one of the major causes of distortion of the aquatic ecosystem and the reduction of oxygen supplies into and within the environment which can lead to the destruction of wildlife.

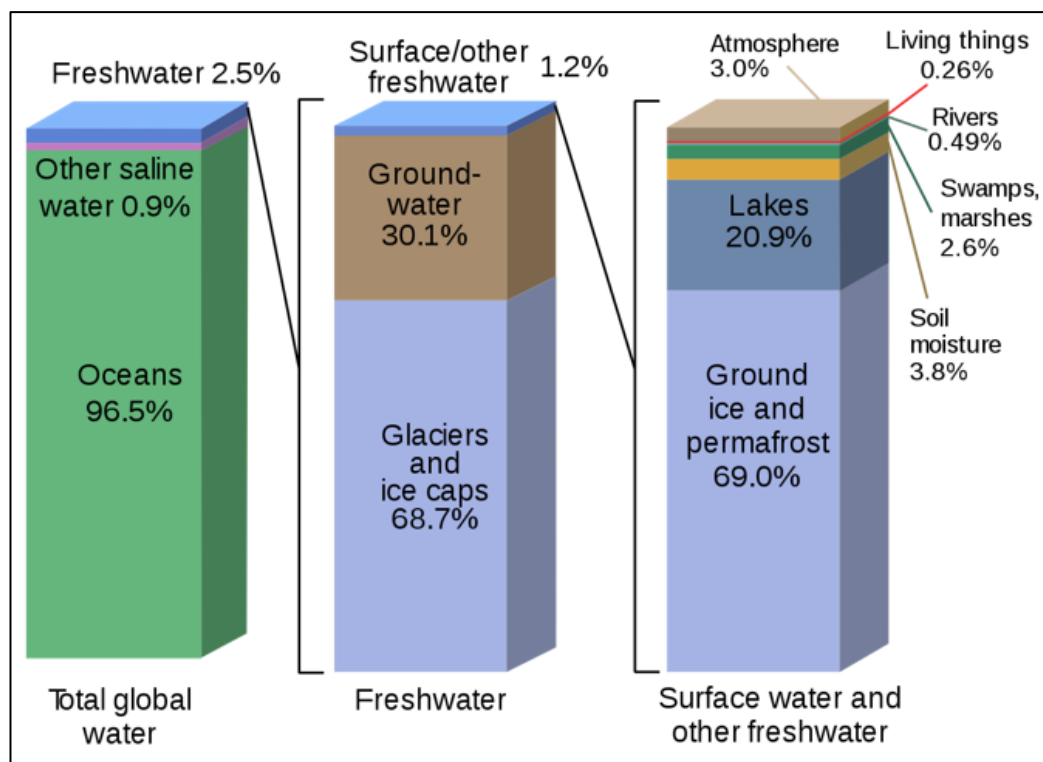


**Fig. 2.1** Percentage of distribution of water (source; <https://water.usgs.gov/edu/gallery/watercyclekids/earth-water-distribution.html>)

### 2.1.1 Surface water pollution

Surface water includes water found naturally on the earth's surface. These include all forms of visible water sources such as oceans, rivers, lakes, and lagoons. Surface water constitutes about 98% of all earth's water and approximately 80% of the water used on daily basis (Hoslett *et al.*, 2018). Pollution of surface water is therefore

of major concern. The most contemporary surveys on national water quality have revealed that almost half of the earth's rivers and streams and more than one-third of our lakes are contaminated and unhealthy for drinking, swimming and fishing (Agency, U. S. E. P., 2018). Surface water can be easily contaminated by anthropogenic activities or due to accidental spills because it occupies a very large portion of the earth's surface.

Excess nutrients, chemicals, plastic wastes, pathogens, heavy metals and pesticides are some of the causes of surface water pollution. Excess nutrients may result in harmful algal blooms and hypoxia both in rivers and coastal seas (Borthakur & Singh, 2020). Pathogens in rivers are very toxic and can damage tissues or cells in humans. Chemical pollution increases the risk of cancer, and causes distortion of hormonal systems, reproductive and nervous systems. Surface water pollution is often a result of multiple contaminations by different pollutants.

### **2.1.2 Groundwater pollution**

Groundwater pollution or groundwater contamination describes a situation where pollutants released on the surface of the ground make their way into the groundwater and contaminate it (Pavlidis & Tsihrintzis, 2018). This type of water pollution is referred to as contamination rather than pollution when the pollution occurs naturally due to the presence of a minor and unwanted contaminant.

Groundwater gets polluted when contaminants such as pesticides, fertilizers, and waste leaching from landfills and septic systems make their way into an aquifer, rendering it unsafe for human consumption. Remediation of contaminated groundwater can be difficult and sometimes, impossible, as well as costly. Once polluted, an aquifer may be unusable for decades, or even thousands of years



(Denchak, 2018). Groundwater can also spread contamination far from the original polluting source as it seeps into streams, lakes, and oceans. Groundwater contaminants are conveyed by an aquifer which is an underground layer of permeable rock, sediment, or soil. Just as groundwater generally moves slowly, so do contaminants in groundwater. Because of this slow movement, contaminants tend to remain concentrated in the form of a plume that flows along the same path as the groundwater. The size and speed of the plume depend on the amount and type of contaminant, its solubility and density, and the velocity of the surrounding groundwater.

Groundwater contamination is caused by natural causes or by anthropogenic activities. Chlorides, arsenic, manganese, radionuclides, etc., occur naturally in rock and soils. These chemicals can be leached into groundwater or conveyed by surface runoffs. Improper disposal of hazardous waste, landfills, releases and spills from stored chemicals and petroleum products, surface impoundments, pesticide and fertilizer use, drainage wells, sewers etc., are all ways that groundwater can be contaminated. One of the main causes of groundwater contamination in the United States is the effluent (outflow) from septic tanks, cesspools, and privies (US EPA, 2021). Faecal water can also pollute groundwater. When faecal water which contains pathogens reaches the groundwater, it is polluted with viruses, bacteria and protozoa. This is the principal cause of diseases such as cholera and diarrhoea (Howarth, 2018).

## **2.2 Water treatment methods**

Water remediation has become very essential and different remediation methods have been used in the past. There are many water treatment methods as illustrated in Fig. 2.2. Water treatment methods can be grouped into physical, chemical, and biological processes (Gilca *et al.*, 2020; Nidheesh *et al.*, 2018).

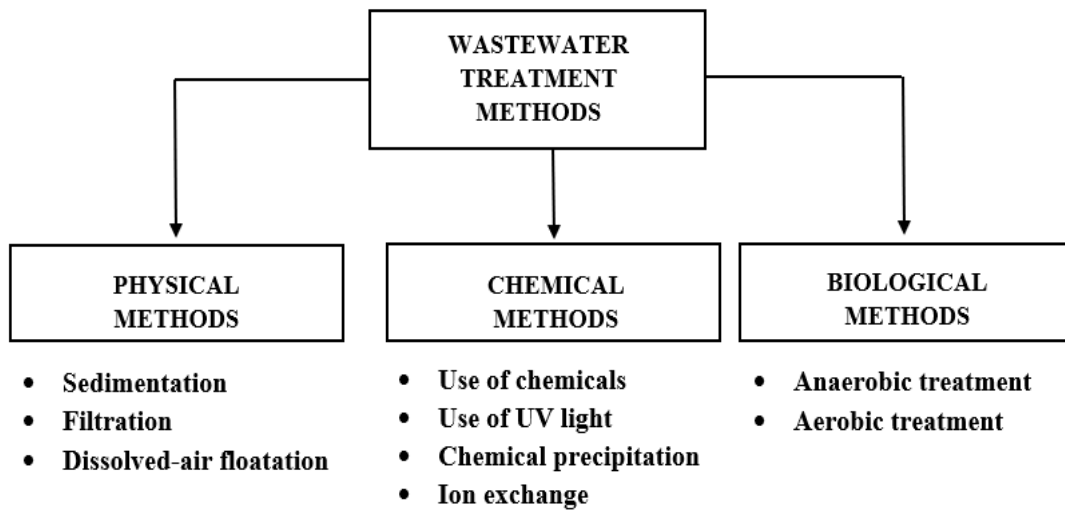


**Fig. 2.2** Classification of water treatment methods for the removal of pollutants with examples (Crini & Lichtfouse, 2019)

### 2.2.1 Physical water treatment methods

The physical water treatment methods include sedimentation, filtration and dissolved air flotation. Sedimentation as a water treatment method involves the setting down of water contaminants against a barrier through their motion caused by forces such as gravity, centrifugal acceleration, or electromagnetism. There are three types of sedimentation (WEF, 2017); the first type of sedimentation involves particles that settle discreetly at constant velocity without flocculation. The sedimentation of grit materials follows this type of sedimentation. The second type of sedimentation involves particles that settle at different velocities and flocculates e.g. iron coagulation. Zone sedimentation is the third type of sedimentation that involves highly concentrated particles which settle as a zone with high velocity such as those found in sludge thickening (Polorigni *et al.*, 2021).

Filtration is a water treatment method involving the passage of contaminated water through a filter medium while retaining the solid particles in the water. Filtration is mostly a pre-treatment method in water treatment. Some membrane technologies employed in water filtration include ultrafiltration, microfiltration, nanofiltration and reverse osmosis (Huang *et al.*, 2015).

The dissolved air flotation (DAF) method of water treatment is used in treating suspended pollutants such as suspended oil and solids (Rocha e Silva *et al.*, 2018). This involves the dissolution of air in contaminated water under pressure and releasing the air under atmospheric pressure in a flotation tank basin. The released air forms tiny air bubbles which adhere to the suspended pollutants and float on the surface of the water. The suspended air bubbles are removed with skimmers.

### **2.2.2 Chemical water treatment methods**

The chemical methods involve the use of chemicals such as chlorine, bromine and ozone for disinfection of contaminated water. The use of ultraviolet light for disinfection is also classified as a chemical method of wastewater treatment. Chlorine is a powerful oxidizing agent which is capable of killing many microorganisms in water. About 64% of water treatment companies still make use of chlorine for water treatment (Djamel Ghernaout, 2018).

Flocculation and coagulation are classified under chemical precipitation. This involves the use of alkalis, acids and coagulants or flocculants such as aluminium ferrous sulphate to precipitate the inorganic impurities from water. This method is referred to as coprecipitation. Precipitation of impurities can also be done by changing the pH or electro-oxidizing potential of the contaminated water (Michael *et al.*, 2006). Chemical precipitation typically involves the addition of precipitating reagents,

adjustment of pH, flocculation, sedimentation and solid-liquid separation. Some precipitating reagents include oxalates, manganese hydroxide, manganese oxide, ferric hydroxide, ferrous hydroxide, calcium carbonate, barium sulphate etc. Ozone is another powerful oxidizing agent used in the treatment of water. Ozone is formed by the combination of an oxygen atom with an oxygen molecule. It is capable of rapidly killing microorganisms found in wastewater. However, the use of ozone is limited in water treatment because ozone is very unstable and disintegrates into oxygen, hence ozone should be generated at the point of application for use in water treatment (Ivanova *et al.*, 2016). The application of ultra-violet (UV) disinfection systems in water treatment in the range of 200 – 400 nm (Vinge *et al.*, 2020) has been in use since 1900. The operating parameters of the newly emerged micro-plasma UV lamp for water treatment as a potential novel UV-based water purifier is recently been under study by researchers (Kheyrandish *et al.*, 2018; Raeiszadeh & Taghipour, 2019). Researchers have also reported that UV radiation as water treatment has advantages which include being very effective in killing bacteria without leaving residues, non-reactive with carbonaceous demand, and effective against the DNA of microorganisms (Ivanova *et al.*, 2016).

Ion exchange is a water treatment technique where at least one unwanted ionic pollutant is exchanged from the solution with another similarly charged ionic substance, electrostatically attached to an immobile solid phase. It is reported that 10 – 40% of natural organic matter is removed after ion exchange (Levchuk *et al.*, 2018).

### **2.2.3 Biological water treatment methods**

Biological wastewater treatment is often employed when the contaminants are biodegradable such as proteins, edible fats and short-chain hydrocarbons. Biological

treatment of water typically involves pretreatment, secondary treatment and disinfection. The pretreatment is chiefly a process of sedimentation to allow for the settlement of larger particles in a series of settling chambers (Samer, 2015).

The secondary biological water treatment involves anaerobic and aerobic treatment. The anaerobic treatment is used where the wastewater contains mostly organic matter. This treatment involves the use of anaerobic microbes which do not require oxygen for their metabolism to treat the wastewater. These microbes degrade the organic contaminants in the wastewater due to metabolism. The aerobic treatment of wastewater employs oxygen-demanding microbes for wastewater treatment. Aerobic biological treatment of wastewater remains stable in all conditions and removes up to 98% of organic contaminants in municipal and industrial wastewater (Samer, 2015).

### **2.3 Oil and petroleum-related pollution**

Total petroleum hydrocarbons (TPH) describe a large family of several hundred chemical compounds that originally come from crude oil (Kuppusamy *et al.*, 2020). In today's developing world, petroleum products and their derivatives are one of the major sources of environmental pollution (Bandura *et al.*, 2017; Mohanakrishna *et al.*, 2019). TPH are currently considered the main source of energy for most industries and daily activities (Varjani & Upasani, 2016). However, TPH are toxic and represent one of the major wide-scale environmental threats to marine and terrestrial environments.

Oil spills cause serious damage to the environment. Spilt crude oil or its products affect aquatic flora and fauna (Paulauskienė *et al.*, 2014). TPH, which are widely applied in the areas of transportation, electricity, production of plastics, etc.,

cause the pollution of surface and groundwater through accidental and anthropogenic activities such as accidental spills, leakages, and industrial activities (Al-hawash *et al.*, 2018). This has inevitably been of major concern over some decades. TPH consist of four major categories of compounds namely; aliphatics, aromatics, resins, and asphaltenes (Adeniji *et al.*, 2017; Ahmed *et al.*, 2020). The short-chain hydrocarbons are usually degraded by microorganisms, but large branched aliphatic chains and aromatic hydrocarbons usually persist in the environment (Ahmed *et al.*, 2020), which highlights the importance of TPH remediation from water bodies. Table 2.1 contains a list of some petroleum product compositions. TPH are classified as priority contaminant because of their nature and versatility in use (Varjani, 2017). Exposure of TPH into the environment occurs either due to human activities or accidentally and cause environmental pollution. These petroleum hydrocarbons (PHCs) can find their way into surface waters or groundwaters through runoffs, leaching or an oil spill. TPH can cause many toxic compounds which are potent immune-toxicants and carcinogenic to humans (Singh Kriti & Subhash, 2014). The release of these compounds into the environment accidentally or by anthropogenic activities leads to environmental pollution and consequent destabilization of the ecosystem (Ahmed *et al.*, 2020). For instance, PHCs in water form a film that could prevent oxygen entry, leading to the death of aquatic organisms (Faustorilla *et al.*, 2017).

Table 2.1: Petroleum product compositions (US Department of Health and Human Services, 1999).

Compound	Carbon Number	Weight Per cent (%)	Fuel Type	Reference
Propane	3	0.01-0.14	Gasoline	LUFT 198
n-Butane	4	3.93-4.70	Gasoline	LUFT 198
		0.12	JP-4	API 1988
Isobutane	4	0.12-0.37	Gasoline	LUFT 198
		0.66	JP-4	API 1993
n-Pentane	5	5.75-10.92	Gasoline	LUFT 198
		1.06	JP-4	API 1993
Cyclopentane	5	0.19-0.58	Gasoline	LUFT 198
		0.05	Crude oil	API 1993
n-Hexane	6	0.24-3.50	Gasoline	LUFT 198
		0.7-1.8	Crude oil	API 1993
		2.21	JP-4	API 1993
2,2-Dimethylbutane	6	0.17-0.84	Gasoline	LUFT 198
		0.04	Crude oil	API 1993
		0.1	JP-4	API 1993
2,3,-Dimethylbutane	6	0.59-1.55	Gasoline	LUFT 198
		0.04-0.14	Crude oil	API 1993
Perylene	20	<0.0001	Diesel	BP 1996
		<0.0024	Fuel oil	BP 1996
Picene	22	0.0000000-0.000083	Diesel	BP 1996
		<0.00012	Fuel oil	BP 1996
Coronene	24	<0.000024	Fuel oil	BP 1996

All the problems arising from TPH as described above have raised the need for TPH remediation in surface and groundwater in which physical and chemical methods such as dissolved air flotation, use of skimmers, barriers, booms, dispersant, or surfactant spray have been employed. Whereas the biological and thermal techniques were based on bioaugmentation, and burning of crude oil, respectively (Barthlott *et al.*, 2020; Liu *et al.*, 2021; Navarathna *et al.*, 2020; Tran *et al.*, 2021). Although these methods have been proven effective, major challenges including the formation of toxic polycyclic aromatic hydrocarbons (PAHs) through oxidation and high cost, have

limited their wide application (Bhattacharya *et al.*, 2018; Bianco *et al.*, 2021; Fuentes *et al.*, 2020).

#### **2.4 Sources of total petroleum hydrocarbons (TPH) pollution**

TPH contamination of marine and terrestrial environments poses a direct and indirect health risk to all forms of life in the affected environment through alteration of population dynamics and disruption of trophic interaction and natural community structure within the ecosystem. TPH pollution of water is largely due to anthropogenic activities such as oil and gas exploration and production, tank leakages, accidental spills in loading and discharging, ballasting and de-ballasting, bunkering, oil tanker incident, and petrochemical industry effluent discharge (Ossai *et al.*, 2020).

#### **2.5 Remediation of TPH from contaminated water**

TPH pollutants or petroleum pollutants are found in both surface water and groundwater. These pollutants are a result of anthropogenic activities such as industrial activities, reservoir leakage and inappropriate waste disposal. Chemical and physical methods are the conventional methods used for the remediation of petroleum contaminants. These methods lead to the production of secondary harmful pollutants in addition to being costly and inefficient. More advanced methods such as electrocoagulation and flocculation have also been employed in the treatment of surface water and groundwater for petroleum pollutants remediation (Mohammadi *et al.*, 2020). These methods have been proven to be more efficient than the conventional water treatment methods but are known to lead to the production of dangerous sludge which is unrecoverable in addition to the high cost of operation.



Nanoparticle adsorption for water remediation is an emerging technology that can be applied using nanomaterials as nanosorbents with excellent adsorption properties due to their large surface area and porosity. The removal of petroleum pollutants from contaminated water by nanosorbents has been reported (Alabresm *et al.*, 2018; Ali *et al.*, 2020). However, these nanosorbents are produced with stabilizing agents which are mostly toxic chemicals. This re-introduces the danger of toxicity as secondary pollutant. Few researchers have reported the use of nanoparticles for the degradation and adsorption of petroleum contaminants for water remediation and even fewer have reported the use of plant-mediated nanoparticles for the removal of petroleum pollutants from contaminated water (Amin *et al.*, 2014; Gautam *et al.*, 2019b; Murgueitio *et al.*, 2018).

Plant-mediated nanoparticles are eco-friendly and very cost-effective. The antioxidants in the plants act as reduction agents by reducing the metal ion precursor to a more stable zerovalent ion thereby preventing agglomeration of the nanoparticles. However, the reaction mechanism involving the combination of plant materials and metal precursors is not yet fully understood.

After treatment of wastewater for remediation of TPH, the wastewater is analyzed to determine the percentage removal of TPH. The TPH method of analysis required by many regulatory agencies is EPA Method 418.1. This method provides a single value of TPH in the environmental media (US Department of Health and Human Services, 1999). However, this method has limitations such as inter-laboratory variations and inherent inaccuracies and it makes use of Freon (CFC-113) as the solvent (Hydrocarbons, 2002). CFC-113 is known to deplete the ozone layer which leads to global warming. For the above reasons, the use of EPA Method 418.1 has been discontinued and replaced by the EPA 8015C, which is a gas chromatographic

method used for the analysis of non-halogenated volatile organic compounds, semi-volatile organic compounds, and petroleum hydrocarbons.

## 2.6 Nitrate pollution of water

Nutrient pollution such as nitrate pollution is the leading type of contamination in these freshwater sources (Denchak, 2018). While plants and animals need these nutrients to grow, they have become a major pollutant due to farm waste and fertilizer runoff. Nitrate pollution has become one of the major concerns in water pollution. Nitrate in nature is normally formed as a denitrification product of nitrogen (Tyagi *et al.*, 2018). Nitrate ( $\text{NO}_3^-$ ) is a product of nitrogen oxidation and hence it is sometimes referred to as “nitrate-nitrogen” ( $\text{NO}_3\text{-N}$ ) because it is a product of nitrogen oxidation. The diagram for the chemical structure of nitrate is shown in Fig 2.3.

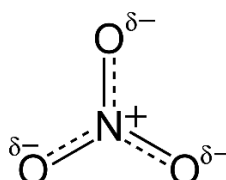


**Fig. 2.3** The chemical structure of nitrate molecule

$\text{NO}_3\text{-N}$  is the main source of nitrogen for plants. It occurs naturally in soil and dissipates when the soil is extensively farmed. Thus, nitrogen fertilizers are applied to replenish the soil. However, these nitrates can be toxic when in high concentrations, especially when they enter the food chain via groundwater and surface water.  $\text{NO}_3\text{-N}$  is an important nutrient that can be found in drinking water but may no longer be safe in drinking water when in higher concentrations than recommended ( $>10 \text{ mg L}^{-1}$ ). Water defilement because of the unreasonable presence of nitrate has become a

significant issue in water quality (Mohseni-Bandpi *et al.*, 2013). High concentrations of nitrate in surface waters present genuine dangers to sea-going ecosystems and can in the end prompt eutrophication (Eneji *et al.*, 2008). Additionally, when they are excessively present in drinking water, they can be carcinogenic to people and aquatic creatures (Kassaei *et al.*, 2011).

High levels of NO<sub>3</sub>-N in water can be a result of runoff or leakage from fertilized soil, wastewater, landfills, animal feedlots, septic systems, or urban drainage. Some studies have suggested an increased risk of cancer, especially gastric cancer, associated with dietary NO<sub>3</sub>-N exposure in larger concentrations than recommended (Ward *et al.*, 2018). Under the Safe Drinking Water Act, the federal maximum contaminant level goal (MCLG) and the maximum contaminant level (MCL) for nitrate are both 10 mg L<sup>-1</sup> (Eisenbrand *et al.*, 1980; Pennino *et al.*, 2017; Ward *et al.*, 2018). Nitrate concentrations above 10 mg L<sup>-1</sup> cause infant methemoglobinemia or blue baby syndrome (Chaudhry FN, Malik MF, 2017). Hence, different procedures including ion exchange or reverse osmosis, biological denitrification, electrocatalysis, and chemical reduction processes are utilized for treating nitrate (Eneji *et al.*, 2008).

## **2.7 Sources of nitrate pollution**

Nitrate contamination of drinking water supplies, particularly groundwater, principally because of agrarian activities (including too much application of inorganic nitrogenous fertilizers), wastewater treatment, and oxidation of nitrogenous by-products in human and animal excreta including in septic tanks, has become a basic worldwide issue leading to nitrogen pollution of water (Pennino *et al.*, 2017). Fig. 2.4 summarizes the sources of nitrate pollution in water.

The expanding use of fake composts, waste disposal, (especially from animal cultivation), and changes in land use are the fundamental factors liable for the increase in nitrate levels in groundwater supplies in recent years (Karanasios *et al.*, 2010). Since nitrate is exceptionally dissolvable in water, excess nitrate can find its way into surface and groundwater, thereby diminishing the water quality (Weigelhofer *et al.*, 2018). Septic tank leakage, agricultural runoffs and wastewater effluents are also some of the ways nitrates find their way into water bodies.

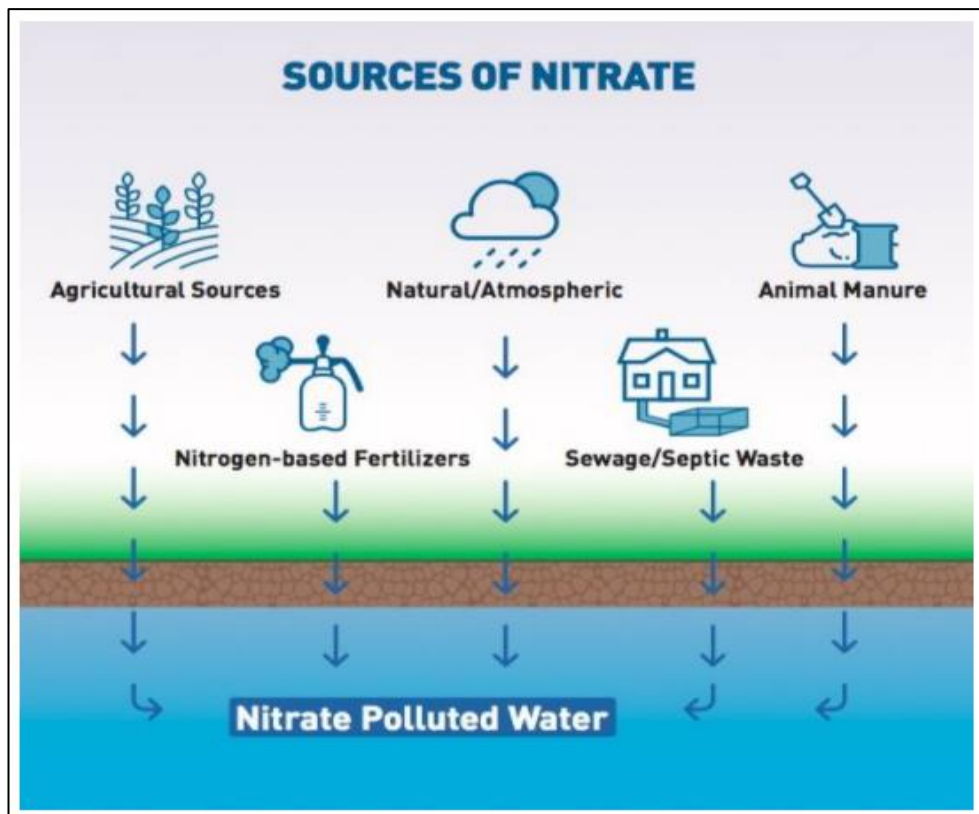


**Fig. 2.4** Diagram showing sources of nitrate pollution (Willis, 2020)

Researchers have successfully used methods such as the use of nitrogen and oxygen stable isotopes to assess the primary sources of nitrate and its migration and transformation in river water. For example, in Xiangshan Bay of Zhejiang Province, the primary nitrate sources were manure and septic waste, and the nitrification degree

in the upper and lower reaches of the bay varied due to different water retention times, which changes the spatial distribution of nitrate in the water body (Yang *et al.*, 2018). In another study, the  $\delta^{15}\text{N}$  and  $\delta^{18}\text{O}$  isotopes of nitrate were a tool used to reveal the sources of nitrate in water bodies in the Nala watershed, at a sugarcane planted area in Guangxi, China. The study revealed that soil nitrate and chemical fertilizer collectively contributed 52.71 % in July 2020 and 57.70 % of nitrate in December 2020, to the water sources within the watershed, respectively. Thus reducing the use of chemical fertilizer in agricultural planted areas provides the key to controlling nitrate pollution (Jin *et al.*, (2020). In an attempt to identify sources of nitrate as a pre-requisite for the development of aquifers, Jia *et al.*, (2020) found out that none of the suspected pollutant sources could account for the unusually high levels of nitrate observed in the groundwater (locally > 850 mg/L). The authors, however, found that isotopic evidence demonstrated that the centrally located Jijiahe Reservoir and Shidi River was a major source of aquifer recharge in the area most seriously affected by nitrate, and was, therefore, an obvious conveyance of the contamination (Jia *et al.*, 2020).

## **2.8 Remediation of nitrate from contaminated water**

Some nitrate removal methods reported by researchers include ion-exchange (Rezvani *et al.*, 2017), electrodialysis (Sharma & Sobti, 2012), reverse osmosis (Rezvani *et al.*, 2017), chemical denitrification (Fanning, 2000), biological denitrification (Ding *et al.*, 2019), electro-dialysis and use of adsorbents (Mohseni-Bandpi *et al.*, 2013)

However, these techniques have shown drawbacks due to high cost, long-term treatment, difficulty in reducing the concentration of pollutants to regulated levels, and the ability to reach the contaminant in the subsurface (Alimentaria, 2018; Schrick *et*